Proceedings of the 2007 IEEE/RSJ International
Conference on Intelligent Robots and Systems
San Diego, CA, USA, Oct 29 - Nov 2, 2007

Dynamics Modeling and Parameter Identification for Autonomous Vehicle Navigation

Kristijan Maček*, Konrad Thoma*, Richard Glatzel*, Roland Siegwart*

*Swiss Federal Institute of Technology Zurich, Switzerland
email: {kristijan.macek@mavt, thomak@student, glatzelr@student, roland.siegwart@mavt}.ethz.ch

Abstract— **This paper focuses on development of a dynamic model for an Ackermann-like vehicle based on a static tire-road friction model and laws of technical mechanics. The model takes as input the steering angle of the wheels in front and the rotational velocities of the drive wheels in the back of the vehicle. It delivers a 3-DOF output in terms of *CoG* vehicle velocity, body slip angle and the yaw rate of the vehicle in the x-y plane, as well as estimates on the forces acting on the system. It is suitable for modeling dynamic vehicle regimes in e.g. overtaking maneuvers/obstacle avoidance and lane-keeping, enabling active steering control by stabilizing the dynamics of the vehicle. The physical model description is based on previous works combined with a suitable friction model that is tractable in practice. Experimental verification of the obtained model is given for the Smart testing vehicle platform, where a separate analysis is done for directly measured as opposed to estimated/optimized parameters of the model.**

I. Introduction

In order to develop stabilizing control laws in dynamic vehicle regimes, a vehicle model that takes dynamics into account is developed in this paper. The model is suitable for lane-keeping control and obstacle avoidance maneuvers when lateral dynamic effects based on wheel slip come into place, i.e at increased vehicle speeds, steering angles and decreased road friction. In future work, this model will be used for the lane-keeping control and obstacle avoidance of the Smart test vehicle for autonomous vehicle navigation in our research [1], aiming at improving vehicle traffic safety.

A vehicle can be analyzed as consisting of five individual subsystems: one vehicle body and four wheels. All the five bodies can in general move freely with respect to each other in six degrees of freedom. Without further simplification the dynamics of a vehicle model would therefore consist of thirty differential equations. However, for control purposes this is neither necessary nor efficient. The existing models cope with this problem by simplifying the model architecture as much as possible while still satisfying the requirements of the model. The simplest solution found in literature is the one-track bicycle model well described by Mitschke in [2]. This model combines the front and rear wheels respectively and treats the vehicle as a bicycle. It describes the vehicle motion in three degrees of freedom (x-y position and yaw rate). More accurate models can be found in [3] and [4] which are four wheel models describing also the pitch and roll movements of the vehicle (five DOF).

For the lane-keeping control, our model is required to generate an accurate prediction of the yaw rate and the longitudinal/lateral acceleration of the vehicle, therefore the calculation of the pitch and roll rate is not necessary and will not be considered here. In consequence, a four wheel three degrees of freedom model is derived, which describes the motion of the car in the x- and y- direction on a horizontal plane and the rotation about the z-axis normal to it.

In Sec. II, the architecture of the model is presented, with each segment of the model analyzed in detail. The vehicle model proposed follows closely the derivation of [5] which is general for simulation of behavior of passenger cars. In Sec. III, the procedure to measure and estimate the parameters of the model is given. The relevant unknown parameters of the model are identified by an optimization routine. The model/parameter validation is based and validated on real vehicle data, where a good fit and realistic estimation of the dynamic vehicle behavior is observed, followed by conclusions in Sec. IV. The contribution of the paper can be found mainly in combining an existing systematic vehicle dynamic model derivation with a choice of a friction model that suits well the vehicle behavior tested on real data and is still simple enough for control purposes. Furthermore, a systematic methodology for model parameter measurement and estimation is presented.

II. Vehicle model

A. Model Architecture

As mentioned earlier, the dynamic model developed here consists of five connected subsystems: one vehicle body and four wheels, which are rigidly coupled to the vehicle body. The model is symmetrical about the vehicle body's longitudinal axis. The rear wheels, which are driven by a torque, cannot be steered and are therefore aligned with the vehicle body's longitudinal axis. The front wheels can be steered according to the Ackermann steering model and the vehicle motion is constrained to horizontal movements only.

As shown in Fig. 1 different coordinate systems for all subsystems are defined with respect to an inertial (*In*) coordinate system, which is defined as a fixed system in which the x- and y- axis describe a horizontal plane and the z-axis points upwards. The center of gravity (*CoG*) coordinate system is associated with the vehicle body and has its origin in the *CoG* of the total system (i.e. vehicle body plus the five wheels). Each wheel has its own (*W*) coordinate system. The wheels always touch the level horizontal plane described by the x_{In}- and y_{In}-axis in one single point (Wheel Ground

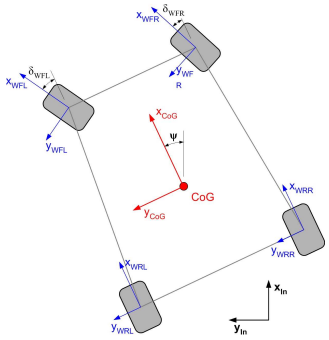

Fig. 1. Coordinate Systems: *In* - Inertial, *CoG* - Center of Gravity, *W* - Wheel.

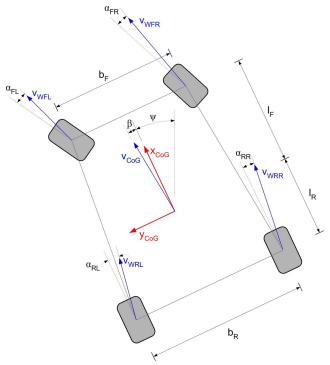

Fig. 2. Geometry and defined velocities of the vehicle.

Contact Points). Relative to the *CoG*-system the wheels are allowed to rotate freely about their rotational axis y_W. The steering angles $\delta_{W_{FL}}$ and $\delta_{W_{FR}}$ of the front wheels and the driving torque T_{Drive} that acts on both rear wheels are the physical inputs to the vehicle.

B. Vehicle kinematics

1) Vehicle Body Kinematics: The velocity of the *CoG* in the *CoG*-system is defined by:

$$\overrightarrow{{}_c v_{CoG}} = \begin{bmatrix} v_{CoG} \cdot \cos(\beta) \\ v_{CoG} \cdot \sin(\beta) \end{bmatrix} \tag{1}$$

Here v_{CoG} is the absolute value of the velocity and β is the angle between the x-axis of the *CoG*-system and the velocity vector as shown in Fig. 2. β is known as the body side slip angle. Transformation of ${}_c v_{CoG}$ to the *In*-system yields:

$$\begin{aligned} \overrightarrow{{}_i v_{CoG}} &= \begin{bmatrix} \cos\psi & -\sin\psi \\ \sin\psi & \cos\psi \end{bmatrix} \cdot \overrightarrow{{}_c v_{CoG}} \\ &= \begin{bmatrix} v_{CoG} \cdot \cos(\beta+\psi) \\ v_{CoG} \cdot \sin(\beta+\psi) \end{bmatrix} \end{aligned} \tag{2}$$

where the yaw angle ψ is the angle between the *In*-system and the *CoG*-system. The acceleration ${}_i a_{CoG}$ of the *CoG* is derived in the *In*-system ([5](p.261)):

$$\begin{aligned} \overrightarrow{{}_i a_{CoG}} = v_{CoG}(\dot\beta+\dot\psi) \begin{bmatrix} -\sin(\beta+\psi) \\ \cos(\beta+\psi) \end{bmatrix} + \\ + \dot v_{CoG} \begin{bmatrix} \cos(\beta+\psi) \\ \sin(\beta+\psi) \end{bmatrix} \end{aligned} \tag{3}$$

Transforming the ${}_i a_{CoG}$ into the *CoG*-system is done by rotating the vector about ψ around the z_{In}-axis:

$$\overrightarrow{{}_c a_{CoG}} = v_{CoG}(\dot\beta+\dot\psi) \begin{bmatrix} -\sin\beta \\ \cos\beta \end{bmatrix} + \dot v_{CoG} \begin{bmatrix} \cos\beta \\ \sin\beta \end{bmatrix} \tag{4}$$

with additional notation ${}_c a_{CoG,x} \equiv a_x$ and ${}_c a_{CoG,y} \equiv a_y$.

2) Wheel Kinematics: The wheel ground contact point velocity is defined as the velocity of the ground contact point of each wheel not taking into account the rotational speed of the wheel [5] (p.226), representing a stationary point with respect to the vehicle body ([6](pp.68)):

$$\overrightarrow{{}_c v_{w_n}} = \overrightarrow{{}_c v_{CoG}} + \begin{bmatrix} 0 \\ 0 \\ \dot\psi \end{bmatrix} \times \begin{bmatrix} x_n \\ y_n \\ 0 \end{bmatrix} \tag{5}$$

The wheel velocities then depend on v_{CoG}, the yaw rate $\dot\psi$, and the geometry of the vehicle, where x_n and y_n are the coordinates of the four wheel ground contact points, $n = 1, \ldots, 4$, given in the CoG-system. The geometry of the car is shown in Fig. 2. The lengths and widths l_F, l_R, b_R, b_R describe the exact position of each wheel ground contact point with respect to CoG. The four wheel velocities are given by:

$$\overrightarrow{{}_c v_{w_{FL,R}}} = \begin{bmatrix} v_{CoG}\cos\beta \mp \dot\psi \frac{b_F}{2} \\ v_{CoG}\sin\beta + \dot\psi l_F \end{bmatrix} \tag{6}$$

$$\overrightarrow{{}_c v_{w_{RL,R}}} = \begin{bmatrix} v_{CoG}\cos\beta \mp \dot\psi \frac{b_R}{2} \\ v_{CoG}\sin\beta - \dot\psi l_R \end{bmatrix} \tag{7}$$

The tire side slip angle α of each wheel is defined similar to the vehicle body side slip angle β. α is the angle between the wheel axis x_{w_n} and the wheel velocity v_{w_n} as shown in Fig. 3. The four α's are calculated by:

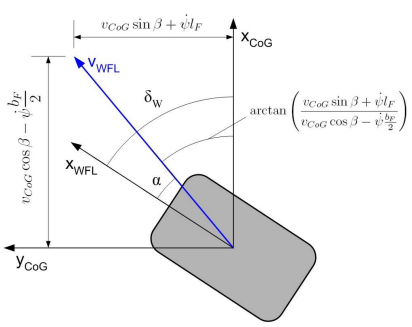

Fig. 3. Side slip angle (given for the front left tire).

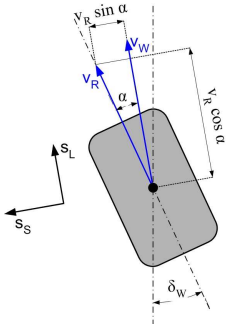

Fig. 4. Wheel slip.

$$\alpha_{FL,R} = \delta_{W_{FL,R}} - \arctan\frac{v_{CoG}\sin\beta + \dot\psi l_F}{v_{CoG}\cos\beta \mp \dot\psi\frac{b_F}{2}} \tag{8}$$

$$\alpha_{RL,R} = -\arctan\frac{v_{CoG}\sin\beta - \dot\psi l_R}{v_{CoG}\cos\beta \mp \dot\psi\frac{b_R}{2}} \tag{9}$$

The wheel equivalent velocity of each wheel, v_{R_n}, is given by the rotational speed of the wheel ω_n and the effective wheel radius, r_{eff} [5](pp.249-250):

$$v_{R_n} = \omega_n \cdot r_{eff} \tag{10}$$

where its direction is the positive x-direction of the wheel coordinate system, describing motion of the wheel if it rolled perfectly on the road.

3) Wheel Slip Calculation: The three expressions for v_w, α and v_R are now combined in the slip equations. The slip is a normalized description of the tire movement relative to the road and is depicted well by Burckhardt in [7]. This relative movement is solely responsible for the tire friction forces and is therefore important for the friction forces calculation. The longitudinal slip s_L is defined in the direction of v_w and describes the relative movement in forward direction. The side slip s_S is defined perpendicular to v_w and describes the relative movement in side direction as shown in Fig. 4. The two slip equations are given in Tab. 11 ([5](p.237)). Burckhardt differentiates between the driving vehicle and the braking vehicle, thus the slip stays always between -1 and 1.

	Braking $v_R \cos\alpha \leq v_W$	Driving $v_R \cos\alpha > v_W$
Longitudinal slip	$s_L = \frac{v_R \cos\alpha - v_W}{v_W}$	$s_L = \frac{v_R \cos\alpha - v_W}{v_R \cos\alpha}$
Side slip	$s_S = \frac{v_R \sin\alpha}{v_W}$	$s_S = \tan\alpha$

(11)

C. Vehicle dynamics

The dynamics of the system can be derived using the principles of linear and angular momentum in two-dimensions for the vehicle body and the four wheels ([6](pp.68)).

1) Vehicle Body Dynamics: According to the principle of linear momentum, the acceleration of the car is determined by the sum of all forces ${}_cF_i$ acting upon it:

$$\sum_{i=1}^{k} \overrightarrow{{}_cF_i} = m_{CoG} \cdot \overrightarrow{{}_ca_{CoG}} \tag{12}$$

The rotational motion of the wheels is neglected here, thus the only rotation allowed by the model architecture is the yaw motion around the z-axis, with T_i being the torques induced by the forces acting on the car (angular momentum):

$$\sum_{i=1}^{l} T_i = J_z \cdot \ddot{\psi} \tag{13}$$

2) Wheel Dynamics: The torque produced about the y-axis of each individual wheel is the engine torque T_{Drive}, which is for the front wheels equal to zero and for the rear wheels counter-balanced by the longitudinal friction forces F_{WL_n} on each wheel:

$$T_{drive_n} = J_{W_n} \dot{\omega}_n + r_{eff} \cdot F_{WL_n} \tag{14}$$

D. Forces description

The most important forces for the dynamics of the vehicle are the friction forces which are generated at the tire/road contact area ([8](p.17)). All the relevant forces for the model acting horizontally upon the system are shown in Fig. 5.

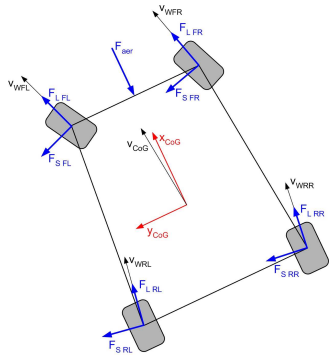

Fig. 5. Forces: F_L (longitudinal) and F_S (lateral) friction forces, F_{aer} the aerodynamic force.

1) Aerodynamic Force: The aerodynamic resistance due to the vehicle's motion through the air is the major braking force in the model and is aligned with the x_{CoG} direction of the car:

$$\overrightarrow{{}_cF_{aer}} = -sgn(v_{CoG}) \cdot c_{aer} A_L \frac{\rho_{Air}}{2} \cdot v_{CoG}^2 \cdot \overrightarrow{{}_ce_x} \tag{15}$$

with ρ_{Air} being air density, c_{aer} aerodynamic constant and A_L the effective aerodynamic surface of the vehicle.

2) Normal Forces: The normal forces are calculated at each wheel ground contact point in the positive z_w direction. Due to the asymmetry of the vehicle body along the vehicle body's lateral axis the normal forces differ already with no motion of the car and become larger at the rear wheels while accelerating and larger at the outside wheels while in a turn. The approach of [5] (pp.306-308) takes into account the shifting of the wheel load while accelerating or driving in a turn. Assuming no suspension and roll or pitch motion, the

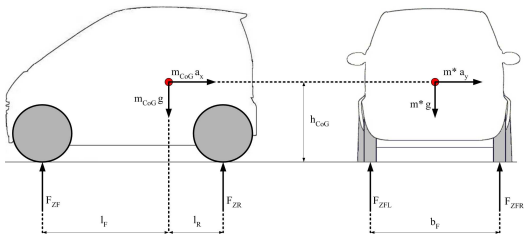

Fig. 6. Normal Forces Calculation.

dependencies of the normal forces on the longitudinal and lateral accelerations, a_x and a_y, can be calculated separately. By balancing different loads on axles due to longitudinal acceleration and furthermore axle load shift due to driving in a turn (see Fig. 6), the torque balance at the front left contact point yields:

$$F_{ZFR} = \frac{1}{2} m_{CoG} \cdot \left(\frac{l_R}{l} g - \frac{h_{CoG}}{l} a_x \right) + \tag{16}$$
$$+ m_{CoG} \cdot \left(\frac{l_R}{l} g - \frac{h_{CoG}}{l} a_x \right) \cdot \frac{h_{CoG} \cdot a_y}{b_F \cdot g}$$

where similar expressions can be derived for other normal forces as well.

3) Friction Forces: The behavior of friction at the tire/road contact area is a highly non-linear phenomenon which is complex to describe. Several approaches to the friction characteristics have been developed. Among these are dynamic friction models of which the LuGre model is among the most promising ([9], [10] and [11]). In contrast, static friction models empirically approximate the tire characteristics and are well studied. Their output are two forces for each wheel which act upon the wheel ground contact point in the direction of v_W, F_L - the longitudinal friction force and perpendicular to it, F_S - the lateral friction force.

4) Burckhardt Friction Model: The static friction model that is used in our system was proposed by Burckhardt in [7]. The model aims at obtaining a realistic relationship between the slip of the tires and the friction coefficients in longitudinal and lateral direction μ_L and μ_S. Two auxiliary parameters s_{Res} and μ_{Res} are introduced:

$$s_{Res} = \sqrt{s_L^2 + s_S^2} \tag{17}$$

$$\mu_{Res} = c_1 \cdot \left(1 - e^{-c_2 \cdot s_{Res}}\right) - c_3 \cdot s_{Res} \tag{18}$$

with calculation of the slips s_L and s_S as explained in Sec. II-B.3.

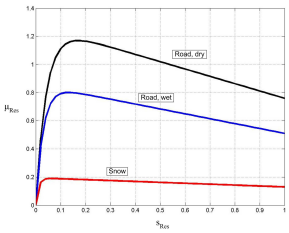

Fig. 7. Friction coefficient characteristics.

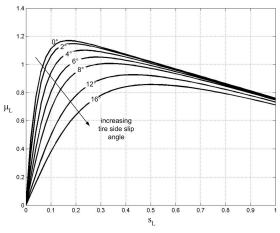

Fig. 8. μ_L dependency on slip s_L and different α side slip angles.

By choosing values for the coefficients c_1, c_2 and c_3 according to different conditions for dry asphalt, wet asphalt and snow, the Fig. 7 shows the resulting friction coefficient as given by Eq. 18. As one can see in Fig. 8, Eq. 18 also provides the dependency of the friction coefficients on the tire side slip angles α.

Now the longitudinal and lateral friction coefficient μ_L and μ_S are calculated by Eq. 19 and the longitudinal and lateral friction forces F_L and F_S are given in Eq. 20 and Eq. 21.

$$\mu_L = \mu_{Res}\frac{s_L}{s_{Res}} \quad , \quad \mu_S = \mu_{Res}\frac{s_S}{s_{Res}} \tag{19}$$

with the longitudinal and lateral friction force being:

$$F_L = \mu_L \cdot F_Z = \mu_{Res} \cdot \frac{s_L}{s_{Res}} \cdot F_Z \tag{20}$$

$$F_S = \mu_S \cdot F_Z = \mu_{Res} \cdot \frac{s_S}{s_{Res}} \cdot F_Z \tag{21}$$

E. Steering

This section deals with the relationship between the angle on the steering column δ_S and the two wheel steering angles $\delta_{W_{FL}}$ and $\delta_{W_{FR}}$ on the front wheels.

1) Steering Column Model: For the derivation of the relationship between δ_S, the steering column angle and δ_W, the steering angle of the hypothetical wheel in the front center, the model used is a static proportional relationship, where i_T is the transmission coefficient of [12](pp.224).

$$\delta_W = \frac{\delta_S}{i_T} \tag{22}$$

2) Ackermann Steering: Since all y-axes of the wheels should intersect in the instantaneous center of motion (*ICM*), the left and right front wheel angles, $\delta_{W_{FL}}$ and $\delta_{W_{FR}}$ are a function of δ_W:

$$\delta_{W_{FL,R}} = \arctan\left(\frac{l}{\frac{l}{\tan\delta_W} \mp \frac{b_F}{2}}\right) \tag{23}$$

F. Summary of the Model

The complete vehicle model combines individual segments elaborated so far. The steering and torque as inputs are propagated through the model, generating forces that produce following outputs: the *CoG*-velocity v_{CoG}, the vehicle body side slip angle β and the yaw rate $\dot{\psi}$ as shown in the equations of motion:

$$\begin{aligned}\dot{v}_{CoG} &= \frac{\cos\beta}{m_{CoG}}\left[\Sigma F_X - c_{aer}A_L\frac{\rho}{2}\cdot v_{CoG}^2\right] \\ &\quad + \frac{\sin\beta}{m_{CoG}}\left[\Sigma F_Y\right]\end{aligned} \tag{24}$$

$$\begin{aligned}\dot{\beta} &= \frac{\cos\beta}{m_{CoG}\cdot v_{CoG}}\left[\Sigma F_Y\right] \\ &\quad - \frac{\sin\beta}{m_{CoG}\cdot v_{CoG}}\left[\Sigma F_X - c_{aer}A_L\frac{\rho}{2}\cdot v_{CoG}^2\right] - \dot{\psi}\end{aligned} \tag{25}$$

$$\begin{aligned}J_Z\ddot{\psi} &= [F_{YFL} + F_{YFR}]\cdot l_F - [F_{YRL} + F_{YRR}]\cdot l_R \\ &\quad + [F_{XFR} - F_{XFL}]\cdot b_F + [F_{XRR} - F_{XRL}]\cdot b_R\end{aligned} \tag{26}$$

where the sum of forces along each coordinate are:

$$\Sigma F_X = F_{XFL} + F_{XFR} + F_{XRL} + F_{XRR} \tag{27}$$

$$\Sigma F_Y = F_{YFL} + F_{YFR} + F_{YRL} + F_{YRR} \tag{28}$$

III. Parameter Estimation and Experimental Model Validation

A. Acquisition of Measurement Data

From the CAN-Bus (Controller Area Network) that is included serially in the Smart vehicle, the following data can be obtained:

- δ_S - steering wheel angle
- w_{FL}, w_{FR} - rotational wheel speed front left/right
- w_{RL}, w_{RR}- rotational wheel speed rear left/right

The IMU300CC-100 is an external inertial measurement unit supplementary integrated in the test vehicle with following measurements taken:

- $\dot{\psi}$ - yaw rate (range $100°/s$, bias $< \pm 2.0°/s$, scale factor accuracy $< 1\%$)
- a_x, a_y - acceleration in the x- and y- direction (range $\pm 2g$, bias $< \pm 30mg$, scale factor accuracy $< 1\%$).

Both sensor systems take measurements at a sample rate of T_s=11ms.

B. Parameter Identification

1) Assured Parameters: In this category of parameters, all natural constants and tabulated values are considered, as well as the car geometry which is given by the drivers manual. The coefficients of the friction model given in Sec. II-D.4 are taken for a dry asphalt road, i.e. $c_1 = 1.2801$, $c_2 = 23.99$ and $c_3 = 0.52$.

2) Measured Parameters:

a) Effective Wheel Radius: r_{eff} is a function of the two static wheel radii r_0 and r_{stat}, where r_0 is the radius of the unloaded wheel and r_{stat} is the compressed wheel radius as the vehicle stands on its four wheels ([5](pp.250)):

$$r_{eff} = r_0 \cdot \frac{\sin(\arccos(\frac{r_{stat}}{r_0}))}{\arccos(\frac{r_{stat}}{r_0})} \tag{29}$$

which for Smart vehicle yields $r_{eff} = 0.273m$.

b) Total Mass of the Smart and x-Position of the CoG: The vehicle was weighted on an industrial scale with an accuracy of 10kg. To find out the x-position of the CoG described by the two lengths l_R and l_F, the law of lever was used:

$$l_F = l \cdot \frac{m_{rear}}{m_{rear} + m_{front}} \;,\; l_R = l \cdot \frac{m_{front}}{m_{rear} + m_{front}} \tag{30}$$

where the results also depend on the number of passengers. For the case of no load: $m = 760kg$, $m_{front} = 330kg$, $m_{rear} = 430kg$, $l_F = 1.025m$, $l_R = 0.787$.

3) Estimated Parameters:

a) Transmission Coefficient - i_{Trans}: The transmission coefficient is important for the car behavior because it determines the magnitude of the wheel steering angles. The initial estimate was i_{Trans}= 15, which is in the range given for other vehicles by [12](pp.224) and was later optimized.

b) Inertial Momenta of the Vehicle Body and the Wheels: To estimate the value of the inertial moment the formula ([12] (p.406)) was used:

$$J_z = 0.1269 \cdot L_T \cdot l \tag{31}$$

where L_T is the total length of the vehicle and l the length between the front and rear axis. This formula gives a result for J_z of about $500kgm^2$.

For the estimation of the inertial momenta of the front wheels, the assumption is that the wheel is a solid disk of radius r=20cm and a mass of m=5kg:

$$J_{W_F} = \frac{1}{2} m \cdot r^2 \tag{32}$$

which yields the inertial momentum of a single front wheel as J_{W_F}=$0.1kgm^2$.

4) Optimization of the Parameters: To optimize the estimated parameters the difference between a set of experimentally measured and modeled outputs is compared. An error function is defined as the sum of all normalized, weighted and squared differences between the five measured and modeled variables:

$$err = \frac{1}{n} \begin{bmatrix} \left(1 \cdot \frac{1}{\llcorner \dot{\psi} \lrcorner}\right)^2 \\ \left(0.5 \cdot \frac{1}{\llcorner a_x \lrcorner}\right)^2 \\ \left(0.5 \cdot \frac{1}{\llcorner a_y \lrcorner}\right)^2 \\ \left(0.5 \cdot \frac{1}{\llcorner \omega_{FL} \lrcorner}\right)^2 \\ \left(0.5 \cdot \frac{1}{\llcorner \omega_{FR} \lrcorner}\right)^2 \end{bmatrix} \cdot \sum_{i=1}^{n} \begin{bmatrix} (\Delta_i(\dot{\psi}))^2 \\ (\Delta_i(a_x))^2 \\ (\Delta_i(a_y))^2 \\ (\Delta_i(\omega_{FL}))^2 \\ (\Delta_i(\omega_{FR}))^2 \end{bmatrix} \tag{33}$$

where the difference for each individual measurement is:

$$\Delta_i(\circ) = (\circ)_{measured}\, i - (\circ)_{modeled}\, i \tag{34}$$

The error of the yaw rate $\dot{\psi}$ is weighted twice as high as the errors of the four other variables because of its importance and the quality of the measurements. The data is normalized with the difference between the maximum and minimum value of each measured parameter over the whole test drive ($\llcorner \dot{\psi} \lrcorner$, $\llcorner a_x \lrcorner$, $\llcorner a_y \lrcorner$, $\llcorner \omega_{FL} \lrcorner$, $\llcorner \omega_{FR} \lrcorner$). The Matlab^{TM} function *fminsearch* is applied in order to search for the minimum of the error function. The optimized parameter values were derived as:

$$i_{Trans} = 28.5576 \;,\; J_z = 1490.3kgm^2 \;,\; J_{W_F} = 0.1071kgm^2$$

which is in good correspondence with the Smart vehicle used, since smaller vehicles types have typically a higher transmission coefficient.

C. Experimental Model Validation

After identifying the unknown parameters of the model and optimizing it with measured data, the model is validated by comparing it to a new test drive of the Smart vehicle. It is expected that the vehicle model follows the measured data without any further optimization. The inputs to the model are shown in Fig. 9, 10 and 11, as front steering wheel angle δ_W (with the estimated steering angles on left and right front wheel δ_{WL}, δ_{WR}) and the rear rotational wheel velocities ω_{RL}, ω_{RR}, respectively. Peak differences in rear wheel velocities indicate that the driving regime is dynamic. Note that the wheel dynamics is induced with the drive torques on rear axis as explained in Sec. II-C.2, however, the torque quantities cannot be measured directly. They can only be estimated in a forward manner by an additional model of vehicle engine and transmission or in a backward manner according to Eq. 14, therefore the rear wheel velocities are considered as direct inputs here and represent the driving quantities.

In Fig. 14, 15 and 16 the yaw rate $\dot{\psi}$ and accelerations a_x and a_y are given as a comparison between the measured and modeled dynamic variables, since they can be directly measured by the IMU unit. For the given precision of the IMU, the model errors are: $|\Delta_{max}|_{\dot{\psi}} = 6.7°/s$,

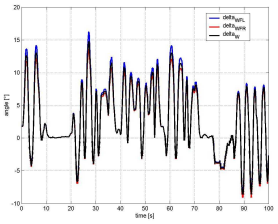

Fig. 9. Measured input steering angle δ_W and estimated left and right front wheel angles δ_{FL} and δ_{FR}.

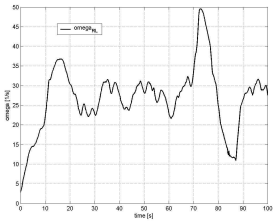

Fig. 10. Measured input wheel velocity rear left ω_{RL}.

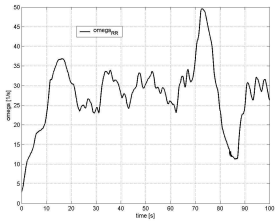

Fig. 11. Measured input wheel velocity rear right ω_{RR}.

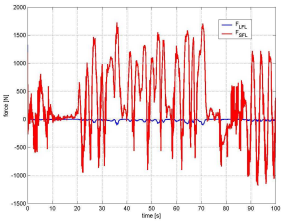

Fig. 12. Estimated wheel forces front left, longitudinal $F_{L_{FL}}$ and lateral $F_{S_{FL}}$.

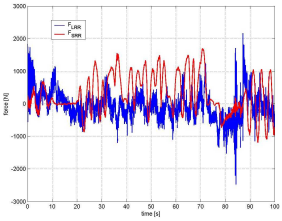

Fig. 13. Estimated wheel forces rear right, longitudinal $F_{L_{RR}}$ and lateral $F_{S_{RR}}$.

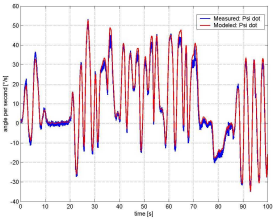

Fig. 14. Estimated and measured yaw rate $\dot{\psi}$.

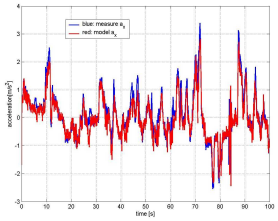

Fig. 15. Estimated and measured acceleration in the x-direction a_x.

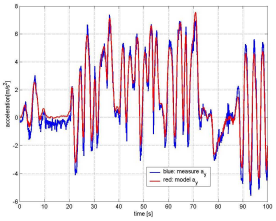

Fig. 16. Estimated and measured acceleration in the y-direction a_y.

$\sigma_{\dot{\psi}} = 2.3°/s$, $|\Delta_{max}|_{a_x} = 0.71m/s^2$, $\sigma_{a_x} = 0.33m/s^2$ and $|\Delta_{max}|_{a_y} = 1.42m/s^2$, $\sigma_{a_y} = 0.74m/s^2$. As can be seen, the measured and modeled data correspond well, with maximal model deviations $|\Delta_{max}|$ due to peaks of highly dynamic regime. The estimated forces on the front left wheel of Fig. 12 show that the lateral force $F_{S_{FL}}$ is considerable and changes direction according to the steering angle. The longitudinal force $F_{L_{FL}}$ at this wheel is small negative or close to zero due to the small wheel inertia and net rolling resistance, opposing the longitudinal motion. The estimated longitudinal force of the rear right wheel $F_{L_{RR}}$ of Fig. 13 is in contrast to $F_{L_{FL}}$ much bigger since it represents one of the two driving forces exerted on the vehicle by the engine and transmission, changing from the acceleration phases (positive) to the braking phases (negative). The overall magnitudes of the forces also correspond well to those found in other literature ([13], [2]) taking into account the scale of the car class. The developed dynamic model will be used for feed-forward trajectory simulation within a control scheme which relies also on the on-line feedback action to account for model inaccuracies.

IV. Conclusion

In this work a 3DOF dynamic vehicle model was developed describing the motion of vehicle in horizontal plane by considering lateral and longitudinal body dynamics and friction forces exerted by the ground surface acting on the vehicle. A detailed analysis included identification of all the relevant parameters of the model, either directly measured or estimated. An experimental verification based on comparison of the model output and measured data of a test vehicle proved a good correlation and validity of the model. Future work will include applying the model for lane-keeping and obstacle avoidance control of the vehicle and automatic switching of friction model coefficients based on different ground surfaces.

V. Acknowledgments

The authors would like to thank their colleague Sascha Kolski for his help in acquiring experimental vehicle data.

References

[1] *"http://www.smart-team.ch"*.
[2] M.Mitschke, *Dynamik der Kraftfahrzeuge, Band C: Fahrverhalten*, Springer, 2 edition, 1990.
[3] H.Junjie, D.A.Crolla, M.C.Levesley, and J.W.Manning, "Integrated active steering and variable torque distribution control for improving vehicle handling and stability," *Vehicle Dynamics and Simulation 2004*, pp. 107–116, 2004.
[4] M.Selby, W.J.Manning, M.D.Brown, and D.A.Crolla, "A coordination approach for dyc and active front steering," *Vehicle Dynamics and Simulation 2001*, pp. 49–55, 2001.
[5] U.Kiencke and L.Nielsen, *Automotive Control Systems*, Springer, 2000.
[6] J.H.Jr.Williams, *Fundamentals of Applied Mechanics*, John Wiley & Sons, Inc., 1996.
[7] M.Burckhardt, *Fahrwerktechnik: Radschlupf-Regelsysteme*, Vogel Fachbuch, 1993.
[8] M.Mitschke, *Dynamik der Kraftfahrzeuge, Band A: Antrieb und Bremsung*, Springer, 3 edition, 1995.
[9] C.Canudas de Wit, H.Olsson, and K.J.Astroemand P.Lischinsky, "A new model for control of systems with friction," *IEEE Transactions on Automatic Control*, vol. 40, no. 3, 1995.
[10] X.Claeys, J.Yi, L.Alvarez, R.Horowitz, and C.Canudas de Wit, "A dynamictire/road friction model for 3d vehicle control and simulation," in *IEEE Intelligent Transportation Systems*, 2001, pp. 483–488.
[11] M.G.Villella, "Nonlinear modeling and control of automobiles with dynamic wheel-road friction and wheel torque inputs," M.S. thesis, Georgia Institute of Technology, 2004.
[12] J.Reimpeland J.W.Betzler, *Fahrwerktechnik: Grundlagen*, Vogel Verlag, 4 edition, 2000.
[13] U.Kiencke and L.Nielsen, *Automotive Control Systems*, Springer, 2 edition, 2005.